

2-Methyl-2,4-pentanediol gas sensor properties of nano-SnO₂ flat-type coplanar gas sensing arrays at low detection limit

CHAO ZHU¹, KAIJIN HUANG^{1,2,3,*}, FANGLI YUAN², CHANGSHENG XIE¹

¹State Key Laboratory of Materials Processing and Die & Mould Technology, Huazhong University of Science and Technology, Wuhan 430074, P.R. China

²State Key Laboratory of Multiphase Complex Systems, Institute of Process Engineering, Chinese Academy of Science, Beijing 100190, P.R. China

³State Key Laboratory of Advanced Technology for Materials Synthesis and Processing, Wuhan University of Technology, Wuhan 430070, P.R. China

Nano-SnO₂ flat-type coplanar 2-Methyl-2,4-pentanediol (MPD) gas sensor arrays were fabricated by a screen-printing technique based on nano-SnO₂ powders prepared by a hydrothermal method. The results show that the fabricated gas sensor arrays have good MPD gas sensing characteristics, such as good selectivity and response-recovery characteristics. Especially, they can be used for detecting the concentration of MPD gas as low as 1 ppm which is much lower than the legal concentration of 20 ppm or 25 ppm. The good sensing properties indicate that the SnO₂ gas sensor arrays have great potential for on-line or portable monitoring of MPD gas in practical environments.

Keywords: *flat-type coplanar gas sensor arrays; gas sensing properties; low detection limit; 2-methyl-2,4-pentanediol; nano-SnO₂ powders*

© Wroclaw University of Technology.

1. Introduction

2-Methyl-2,4-pentanediol (MPD), with the formula (CH₃)₂C(OH)CH₂CH(OH)CH₃ has many special properties, such as dual lipophilic and hydrophilic, short hydrocarbon chain and high solubility in water over a wide range of temperatures [1]. Because of those special properties, MPD has become a very important compound. MPD is widely used as a chemical intermediate [2], a solvent for perfume and cosmetics [3, 4], an excipient in the formulation [5], an organic additive to promote the phase transition [6], antibacterial and antifungal agent [7], a cryoprotectant [8] and a single most successful agent promoting crystallization of biological macromolecules [1], and so on [9]. MPD is regarded as a high volume chemical (HVC) with production exceeding 0.5×10^6 kg annually in the United States [3].

However, it is worth to notice that MPD is also a toxic compound. Hathaway *et al.* [9] reported that MPD is an irritant of the eyes and mucous membranes and causes narcosis at high level. In detail, when exposed to 50 ppm for 15 min, humans felt slight eye irritation. At 100 ppm for 5 min, humans plainly detected the gas and slight nasal and respiratory discomfort was noted. At 1000 ppm for 5 min, various degrees of eye irritation and throat and respiratory discomfort were noted. Crispe [10] found that only 82 % of the human monocytes still appeared viable after incubation at 3×10^{-1} M of MPD. Nacci *et al.* [11] determined that MPD had exceptionally toxic effect to sperm which had also been confirmed by Cuevas-Urbe *et al.* [8]. Procter [12] reported that MPD could depress the central nervous system and had a toxic action on the kidneys as well as the liver. Spoerl *et al.* [5] ascertained that contact urticaria with systemic symptoms may be caused by open application of MPD 10 %. Therefore, many countries have regulated the occupational exposure limits of MPD gas in

*E-mail: huangkaijin@hust.edu.cn

the workplace. In China, the maximum allowable concentration (MAC) is 20 ppm (100 mg/m³) [13]. And the short term exposure limit (STEL)/ceiling limit for MPD is 25 ppm (125 mg/m³) in the United States [9]. The data indicate that it is worth and necessary to monitor the concentration of MPD gas in the workplace.

MPD has been detected by some conventional measurement systems. Bethel *et al.* [14] used solid-phase micro extraction (SPME) fibers with on-fiber derivatization, gas chromatography-mass spectrometry (GC-MS) and gas chromatography with flame ionization detection (GC-FID) to detect MPD and the reaction products between MPD and OH radical. The GC-FID measurement uncertainty for MPD was less than 5 %. Subsequently, Fourier transform infrared (FTIR) with a 1 cm⁻¹ resolution and GC-FID were used by Magneron *et al.* [3] to the analysis of MPD and the reaction products between MPD and OH radical to reveal the reaction mechanism. Liquid chromatography/mass spectrometry (LC/MS) with electro spray ionization was successfully applied to the analysis of MPD by Saitoh *et al.* [15]. In the study, the limit of detection (LOD) of *m*-aminophenylboronate of MPD with selected-ion monitoring mode was 118.18 fg (about 0.02 ppt). Although those chromatography apparatuses have a low detection limit of ppt level, their use is limited, because the measurements are time-consuming and expensive [16, 17] and require the service of highly-trained operators [18]. Gas sensors have been used successfully to detect many gases, such as alcohols [19], aldehydes [18] and ketones [20], and some inorganic gases [21]. Compared with the conventional measurement systems, gas sensors have many advantages, for instance, they do not require pretreatment on-line operation [22], can operate at relatively low power consumption, and offer high compatibility with microelectronic processing [23–25]. Therefore, it is a good choice to detect MPD using gas sensors. However, to our best knowledge, MPD has not been detected by this promising method. Therefore, the purpose of this work is to develop a gas sensor which could be used as an instrument to detect MPD in the workplace to broaden the application range of gas sensors.

In this paper, the nano-SnO₂ flat-type gas sensor arrays were fabricated by screen-printing technique based on nano-SnO₂ powders prepared by hydrothermal method. The temperature- and concentration-dependent behaviors, dynamic response and selectivity of the developed sensors to MPD were investigated. Based on our work, it is hopeful to develop nano-SnO₂ flat-type coplanar gas sensor arrays which can be used for on-line or portable monitoring of MPD gas in practical environments.

2. Materials and methods

2.1. Fabrication of nano-SnO₂ flat-type coplanar gas sensor arrays

First, the nano-SnO₂ powders were synthesized by hydrothermal method. Then, the nano-SnO₂ powders were ground with some organic compounds including terpineol, butyl carbitol, ethylcellulose, span 85 and di-n-butyl phthalate to get a paste. Next, screen-printing technique was used to print the paste on alumina substrates which had already printed Au electrodes and RuO₂ heaters by the same technology. After sintering, the alumina substrates were welded onto TO-8-003 supports (Yixing City Jitai Electronics) by using gold wires and a welding machine. Finally, the SnO₂ flat-type coplanar gas sensor arrays were fabricated after aging in the air. More details were described in our previous work [26].

2.2. Measurements of gas sensing properties

All the gas sensing properties were studied in a static testing instrument which was developed by our laboratory [27]. The basic measuring circuit of the static testing instrument is similar to the one presented in literature [28, 29]. The accuracy of the test circuit is about ±5%.

The response S is defined by Eq. 1 [21, 28]:

$$S = \frac{R_a}{R_g} \quad (1)$$

where R_a and R_g represent the resistance of the sensors in the air and in the target gas, respectively. The mean response of the four sensors in

each sensor arrays was chosen to be the response of the nano-SnO₂ flat-type coplanar gas sensor arrays. Response time ($t_{response}$) and recovery time ($t_{recover}$) are the times needed for 90 % change in the gas sensor resistance after the tested gas has been injected and removed, respectively [30].

The tests of dynamic response of the nano-SnO₂ flat-type coplanar gas sensor arrays to MPD was conducted by continually exposing the sensor arrays to different concentrations of MPD gas for 2 min and to the air for 2 min, respectively.

3. Results and discussion

3.1. Characterization of nano-SnO₂ powders

The nano-SnO₂ powders synthesized by hydrothermal method are spherical and have a cassiterite structure. The average diameter and the specific surface area of the nano-SnO₂ powders are about 9.2 nm and 143.702 m²/g, respectively [26].

3.2. Gas sensing properties of nano-SnO₂ flat-type coplanar gas sensor arrays

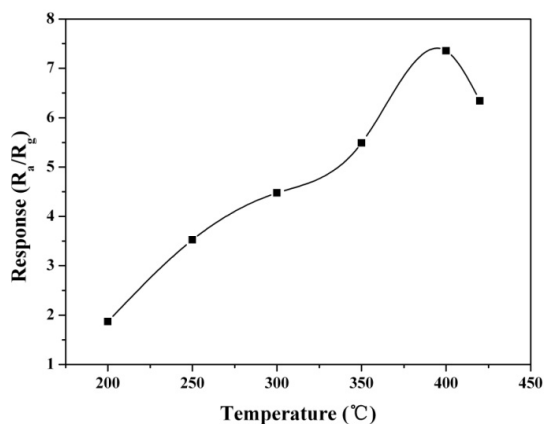


Fig. 1. Response of the nano-SnO₂ flat-type coplanar gas sensor arrays to 100 ppm MPD gas at different operating temperatures.

In order to determine the optimal operating temperature, the gas sensor arrays were used to detect 100 ppm MPD gas at different operating temperatures from 200 °C to 420 °C. The results are shown in Fig. 1. From Fig. 1, it is apparent that

the responses increase with the operating temperatures up to 400 °C where the response reaches the maximum value (7.4). As the temperature continues to rise, the response begins to decrease. This phenomenon can be explained by the adsorption of oxygen molecules. It is well known that the adsorption of oxygen molecules on the gas sensing films has two forms: physisorption and chemisorption, depending on the operating temperature [31]. At lower temperature, physisorption is dominant. Compared with chemisorption, physisorption has weaker ability to trap electrons from the conduction band on the surface. For n-type SnO₂, the thickness of the surface electron depletion layer will be narrower at lower temperature. So, the change of resistance will be smaller when the gas sensors are exposed to reducing gas [27]. Besides, the elevated operating temperature provides the high activation energy to promote the transition from physisorption to chemisorption and the chemical reaction between MPD molecules and the oxygen adsorbates (O_2^- , O^- , O^{2-}) [32–34]. At the same time, with an increase in the operating temperature, the dominating species of chemisorbed oxygen are successively O_2^- , O^- and O^{2-} which is in the same order (from weak to strong) as the ability to give an electron back to SnO₂ conduction band [35]. Therefore, the response increases with the rise in operating temperature. While the basic adsorption reaction ($\frac{1}{2}O_{2(g)} + e^- \rightarrow O_{ads}^-$) is absolutely exothermic [27, 28], the reaction may change when the temperature continues to rise. It means that with rising the operating temperature, the trapped electrons will come back to the conduction band and the thickness of depletion layer will be narrower, which will result in a lower response. On the other hand, at an extremely high temperature, desorption of the adsorbed oxygen is dominant, so the concentration of chemisorbed oxygen decreases and the response of the gas sensor arrays declines [29]. As a result, the response begins to decrease when the operating temperature exceeds 400 °C.

Fig. 2 displays the relationship between the response and MPD gas concentration in the range of 1 ppm to 100 ppm at 400 °C. The response rapidly increases with the rise in MPD gas concen-

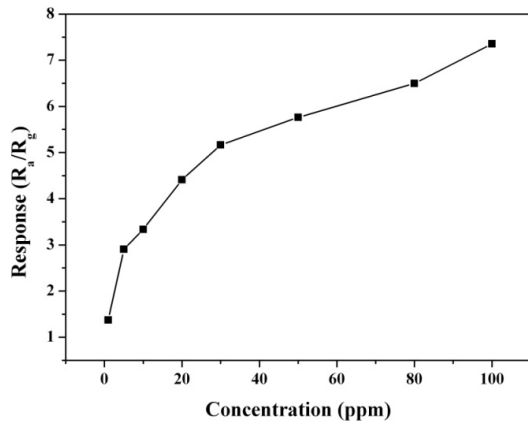


Fig. 2. Response of the nano-SnO₂ flat-type coplanar gas sensor arrays to different concentrations of MPD gas at 400 °C.

tration. The results indicate that the sensors have not reached saturation at 100 ppm under optimal operation temperature (400 °C) [36]. At the same time, the response reaches 4.4 when MPD concentration is 20 ppm, which is the maximum allowable concentration (MAC) of MPD in the workplace in China, indicating the nano-SnO₂ flat-type coplanar gas sensor arrays are suitable for monitoring MPD gas.

For metal oxide semiconductor (MOS) gas sensors, the relationship between the response S and the target gas concentration C , can be described by Eq. 2. In Eq. 2, A and N are constants [37].

$$S = A[C]^N \quad (2)$$

The Eq. 2 can also be rewritten as Eq. 3:

$$\text{Lg}(S) = \text{Lg}(A) + N\text{Lg}(C) \quad (3)$$

It follows from Eq. 3, that the relation between S and C is liner in logarithmic scale. Di-logarithm fit curve of the response and MPD gas concentration in the range of 1 ppm to 100 ppm was carried out, as shown in Fig. 3. In the fitting procedure Eq. 4 was used.

$$\text{Lg}(S) = 0.1739 + 0.3501\text{Lg}(C) \quad (4)$$

The correlation coefficient R is about 0.99374. When $S > 1$ was used as the standard for reliable gas sensing [38], the detection limit of MPD

gas was calculated to be 300 ppb which is much lower than the MAC of MPD in the workplace in China (20 ppm). The low detection limit can be attributed to nanometer-size effect of nano-SnO₂ gas sensing material. The average size of SnO₂ powders is about 9.2 nm [26] and the Debye length (L_d) of SnO₂ powders at the operating temperature is about 3 nm [39, 40]. For that reason, the average size of SnO₂ powders is comparable with $2L_d$. Therefore, the gas response will be promoted much more [40, 41]. In addition, the high specific surface area (143.702 m²/g) [26] provides high surface energy and enough active sites for oxygen ions-MPD molecules reaction to get high responses [34, 42, 43].

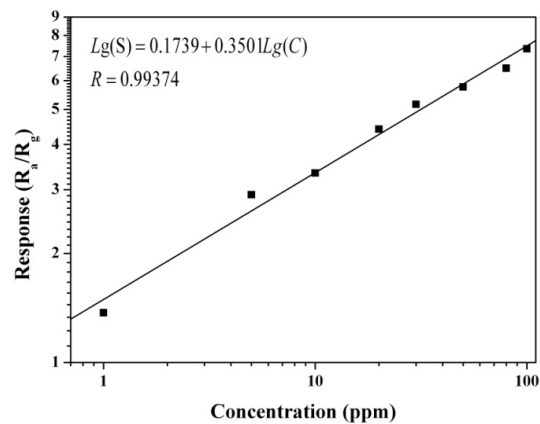


Fig. 3. Di-logarithm fit curve of the responses of the nano-SnO₂ flat-type coplanar gas sensor arrays to different concentrations of MPD gas at 400 °C.

Fig. 4 shows a typical dynamic response of the gas sensors to MPD gas concentrations ranging from 1 ppm to 100 ppm. The output voltage rapidly increases and reaches its equilibrium when a certain amount of MPD gas is injected. Moreover, the equilibrium value is bigger when the MPD gas concentration is higher. At the same time, the drift of baseline in the air after each response-recovery cycle is also noticed and the drift amplitude increases with rising the MPD gas concentration. This phenomenon can be explained by the incomplete desorption of the target gas on the gas sensing films which causes that the recovery time is prolonged [44]. In addition, the response time is 19 s

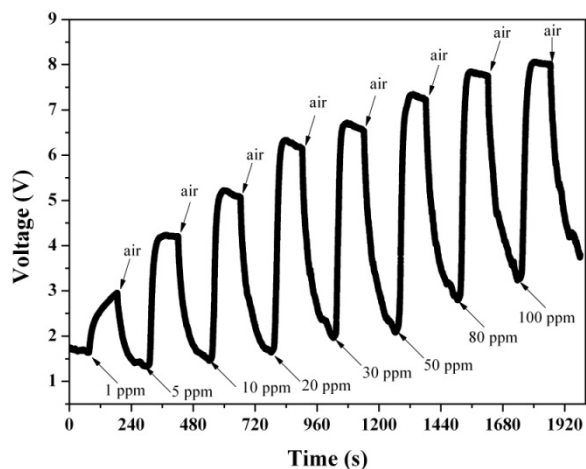


Fig. 4. A typical dynamic response of the nano-SnO₂ flat-type coplanar gas sensor arrays to MPD gas concentrations ranging from 1 ppm to 100 ppm at 400 °C.

and the recovery time is 55 s for 20 ppm MPD gas, indicating the SnO₂ gas sensor arrays have a good response-recovery characteristics to meet the needs of MPD detection.

Obviously, the selectivity is one of the most important properties of gas sensors [45]. Poor selectivity will increase mistaken alarm and so the extensive utilization of the gas sensors will be limited [46]. To research the selectivity of the SnO₂ gas sensor arrays toward MPD gas, five potential interfering gases including ether, formaldehyde, ammonia, xylene and cyclohexane were tested with the SnO₂ gas sensor arrays. All of the gases were tested at an operating temperature of 400 °C with a concentration of 20 ppm (Fig. 5). Obviously, the nano-SnO₂ gas sensor arrays have a better selectivity to MPD in comparison to other interference gases. The similar method for assessment of the selectivity of a sensor was developed by Zhang [47] and Chen [48].

The good selectivity can be well explained by an electron-liberate theory [49], the reducing ability of the test gas [50] (referring to the degree of difficulty of the receiving and losing electrons of the test gas in an oxidation-reduction reaction) and the bond energy of the test gas [51, 52]. Since the operating temperature of the nano-SnO₂ flat-type coplanar gas sensor arrays is 400 °C, O²⁻ is the

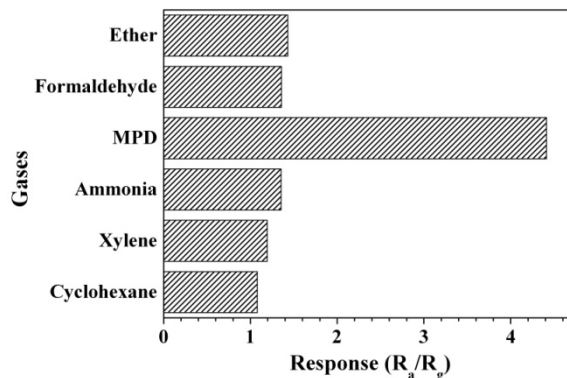
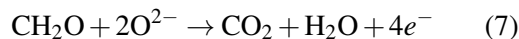
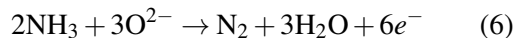


Fig. 5. Responses of the nano-SnO₂ flat-type coplanar gas sensor arrays to 20 ppm of different gases at 400 °C.

dominating species of chemisorbed oxygen on the surface and grain boundaries [50, 53]. The complete oxidation reactions of the test gas are as follows (take MPD (C₆H₁₄O₂), ammonia (NH₃) and formaldehyde (CH₂O) as examples):



The liberated electrons have a great influence on the response of the gas sensor. At the same concentration of the test gas, the more the liberated electrons, the higher the response [49, 50]. So it seems that the order of the response should be xylene (42e⁻) > cyclohexane (36e⁻) > MPD (34e⁻) > ether (24e⁻) > ammonia (6e⁻) > formaldehyde (4e⁻). However, the reducing ability of the test gas should also be considered. The benzene ring in xylene and -cyclohexyl in cyclohexane are stable [35, 50, 54], resulting in the low responses of the gas sensor arrays to xylene and cyclohexane. Due to the fact that methyl is an electron-donating group [35, 53], the response of the gas sensor arrays to xylene is a little higher than that to cyclohexane. The bond energy of H-NH₂ in ammonia (435 kJ/mol) is higher than the bond energy of H-CHO in formaldehyde (364 kJ/mol) [46]. Because of the bond energy, the response of the gas sensor arrays to ammonia is lower than that to formaldehyde which is similar to some reports [51, 52].

Therefore, the response sequence of the gas sensor arrays is: MPD > ether > formaldehyde > ammonia > xylene > cyclohexane, indicating the good selectivity of the nano-SnO₂ gas sensor arrays to MPD gas.

4. Conclusions

The nano-SnO₂ flat-type coplanar gas sensor arrays fabricated by a screen-printing technique based on nano-SnO₂ powders prepared by a hydrothermal method show good gas sensing characteristics, for example, good selectivity and response-recovery characteristics. The most striking result is that the nano-SnO₂ flat-type coplanar gas sensor arrays can be used to detect the concentration of MPD gas as low as 1 ppm which is much lower than the legal concentration of 20 ppm or 25 ppm.

Acknowledgements

This work was supported by the Opening Project (MPCS-2011-D-13) of State Key Laboratory of Multiphase Complex Systems, Institute of Process Engineering, Chinese Academy of Science, and the Opening Project (2012-KF-4) of State Key Laboratory of Advanced Technology for Materials Synthesis and Processing (Wuhan University of Technology). The authors are also grateful to Analytical and Testing Center of Huazhong University of Science and Technology.

References

- [1] ANAND K., PAL D., HILGENFELD R., *Acta Crystallogr. D*, 58 (2002), 1722.
- [2] ZOREBSKI E., DZIDA M., CEMPA M., *J. Chem. Eng. Data*, 53 (2008), 1950.
- [3] MAGNERON I., BOSSOUTROT V., MELLOUKI A., LAVERDET G., LE BRAS G., *Environ. Sci. Technol.*, 37 (2003), 4170.
- [4] KINNUNEN T., HANNUKSELA M., *Contact Dermatitis*, 21 (1989), 154.
- [5] SPOERL D., SCHERER K., BIRCHER A.J., *Dermatology*, 220 (2010), 238.
- [6] SHUL Y.G., OH K.S., YANG J.C., JUNG K.T., *J. Sol-Gel. Sci. Techn.*, 8 (1997), 255.
- [7] KINNUNEN T., KOSKELA M., *Acta Derm-Venereol.*, 71 (1991), 148.
- [8] CUEVAS-URIBE R., YANG H.P., DALY J., SAVAGE M.G., WALTER R.B., TIERSCH T.R., *Zebrafish*, 8 (2011), 167.
- [9] HATHAWAY G.J., PROCTOR N.H., *Proctor and Hughes' Chemical Hazards of the Workplace*, John Wiley & Sons, Hoboken, New Jersey, 2004.
- [10] CRISPE I.N., *Exp. Cell Res.*, 100 (1976), 443.
- [11] NACCI D., JACKIM E., WALSH R., *Environ. Toxicol. Chem.*, 5 (1986), 521.
- [12] PROCTER D.S.C., *S. Afr. Med. J.*, 40 (1966), 1116.
- [13] The Ministry of Health of P.R. China, *Occupational Exposure Limits for Hazardous Agents in the Workplace: Chemical Hazardous Agents (GBZ 2.1-2007)*, People's Medical Publishing House, Beijing, 2007.
- [14] BETHEL H.L., ATKINSON R., AREY J., *J. Phys. Chem. A*, 107 (2003), 6200.
- [15] SAITOH H., GAMOH K., *Bunseki Kagaku*, 51 (2002), 853.
- [16] ALLOUCH A., GUGLIELMINO M., BERNHARDT P., SERRA C.A., LE CALVÉ S., *Sensor. Actuat. B-Chem.*, 181 (2013), 551.
- [17] FREITAS A.M.C., PARREIRA C., VILAS-BOAS L., *J. Food Compos. Anal.*, 14 (2001), 513.
- [18] CHUNG P.R., TZENG C.T., KE M.T., LEE C.Y., *Sensors*, 13 (2013), 4468.
- [19] WANG L.W., KANG Y.F., LIU X.H., ZHANG S.M., HUANG W.P., WANG S.R., *Sensor. Actuat. B-Chem.*, 162 (2012), 237.
- [20] XIAO Y.H., LU L.Z., ZHANG A.Q., ZHANG Y.H., SUN L., HUO L., LI F., *ACS Appl. Mater. Interfaces*, 4 (2012), 3797.
- [21] KHAN Z.H., SALAH N.A., HABIB S.S., AZAM A., EL-SHAHAWI M.S., *Curr. Nanosci.*, 8 (2012), 274.
- [22] UEDA T., UMEDA M., OKAWA H., TAKAHASHI S., *Ionics*, 18 (2012), 337.
- [23] COMINI E., FAGLIA G., SBERVEGLIERI G., PAN Z.W., WANG Z.L., *Appl. Phys. Lett.*, 81 (2002), 1869.
- [24] WISITSORAAT A., TUANTRANONT A., THANACHAYANONT C., PATTHANASETTAKUL V., SINGJAI P., *J. Electroceram.*, 17 (2006), 45.
- [25] MAJUMDER S., HUSSAIN S., BHAR R., PAL A.K., *Vacuum*, 81 (2007), 985.
- [26] HUANG K.J., ZHU C., YUAN F.L., XIE C.S., *J. Nanosci. Nanotechnol.*, 13 (2013), 4370.
- [27] XIE C.S., XIAO L.Q., HU M.L., BAI Z.K., XIA X.P., ZENG D.W., *Sensor. Actuat. B-Chem.*, 145 (2010), 457.
- [28] DONG X.W., QIN L.P., XU J.Q., PAN Q.Y., CHENG Z.X., XING Q., *Curr. Nanosci.*, 4 (2008), 236.
- [29] NIU X.S., DU W.M., DU W.P., *Sensor. Actuat. B-Chem.*, 99 (2004), 399.
- [30] WU Q.H., LI J., SUN S.G., *Curr. Nanosci.*, 6 (2010), 525.
- [31] YANG Z.X., HUANG Y., CHEN G., GUO Z.P., CHENG S.Y., HUANG S.Z., *Sensor. Actuat. B-Chem.*, 140 (2009), 549.
- [32] DONG Y.F., WANG W.L., LIAO K.J., *Sensor. Actuat. B-Chem.*, 67 (2000), 254.
- [33] PATIL L.A., MAHANUBHAV M.D., *B. Mater. Sci.*, 30 (2007), 141.
- [34] WEI A., WANG Z., PAN L.H., LI W.W., XIONG L., DONG X.C., HUANG W., *Chinese Phys. Lett.*, 28 (2011), 080702.
- [35] CHU X.F., ZHOU S.M., ZHANG W.B., SHUI H.F., *Mat. Sci. Eng. B-Solid*, 164 (2009), 65.

- [36] ZHANG L.X., ZHAO J.H., LU H.Q., LI L., ZHENG J.F., LI H., ZHU Z.P., *Sensor. Actuat. B-Chem.*, 161 (2012), 209.
- [37] SHEN Y.B., YAMAZAKI T., LIU Z.F., MENG D., KIKUTA T., *Thin Solid Films*, 517 (2009), 6119.
- [38] XU L., XING R.Q., SONG J., XU W., SONG H.W., *J. Mater. Chem. C*, 1 (2013), 2174.
- [39] OGAWA H., NISHIKAWA M., ABE A., *J. Appl. Phys.*, 53 (1982), 4448.
- [40] GNANASEKAR K.I., RAMBABU B., LANGRY K.C., *Eur. Phys. J.-Appl. Phys.*, 18 (2002), 9.
- [41] LI C.C., LI L. M., DU Z.F., YU H.C., XIANG Y.Y., LI Y., CAI Y., WANG T.H., *Nanotechnology*, 19 (2008), 035501.
- [42] RUMYANTSEVA M.N., GASKOV A.M., ROSMAN N., PAGNIER T., MORANTE J.R., *Chem. Mater.*, 17 (2005), 893.
- [43] LIAO L., LU H.B., LI J.C., HE H., WANG D.F., FU D.J., LIU C., ZHANG W.F., *J. Phys. Chem. C*, 111 (2007), 1900.
- [44] ZHAN S., LI D.M., LIANG S.F., CHEN X., LI X., *Sensors*, 13 (2013), 4378.
- [45] AKSUNER N., HENDEN E., YILMAZ I., CUKUROVALI A., *Sensor. Actuat. B-Chem.*, 166 – 167 (2012), 269.
- [46] LIU Z.T., FAN T.X., ZHANG D., GONG X.L., XU J.Q., *Sensor. Actuat. B-Chem.*, 136 (2009), 499.
- [47] ZHANG Y., XU P.C., XU J.Q., LI H., MA W.J., *J. Phys. Chem. C*, 115 (2011), 2014.
- [48] CHEN M., WANG Z.H., HAN D.M., GU F.B., GUO G.S., *Sensor. Actuat. B-Chem.*, 157 (2011), 565.
- [49] XIANG Q., MENG G.F., ZHANG Y., XU J.Q., XU P.C., PAN Q.Y., YU W.J., *Sensor. Actuat. B-Chem.*, 143 (2010), 635.
- [50] CHU X.F., CHEN T.Y., ZHANG W.B., ZHENG B.Q., SHUI H.F., *Sensor. Actuat. B-Chem.*, 142 (2009), 49.
- [51] WANG X.Q., ZHANG M.F., LIU J.Y., LUO T., QIAN Y.T., *Sensor. Actuat. B-Chem.*, 137 (2009), 103.
- [52] GUO W., DUAN X.C., SHEN Y., QI K.Z., WEI C.Y., ZHENG W.J., *Phys. Chem. Chem. Phys.*, 15 (2013), 11221.
- [53] ZHANG L.X., ZHAO J.H., LU H.G., LI L., ZHENG J.F., ZHANG J., LI H., ZHU Z.P., *Sensor. Actuat. B-Chem.*, 171 – 172 (2012), 1101.
- [54] WONG J.C.S., YATES J.T., *J. Am. Chem. Soc.*, 116 (1994), 1610.

Received 2013-10-28

Accepted 2014-02-01